



CORROSION OF MATERIALS USED FOR CAR EXHAUST SYSTEMS IN ROAD SALT ENVIRONMENT

Karina JAGIELSKA-WIADEREK * , Grzegorz GOLAŃSKI 

Czestochowa University of Technology, Faculty of Production Engineering and Materials Technology. Poland

* Corresponding author, e-mail: k.jagielska-wiaderek@pcz.pl

Abstract

The paper presents the results and analysis of potentiokinetic investigation on materials used in elements of exhaust systems in combustion engine vehicles. The tests were performed for stainless steel X5CrNi18-10 and titanium 3.7035. The resistance to general corrosion and the susceptibility to pitting corrosion was determined for these materials in environments containing chloride ions ranging between 0.2÷1.0M. Moreover, the susceptibility to repassivation was examined. The performed tests showed high electrochemical stability of titanium and lack of the susceptibility to pitting corrosion in the applied environmental conditions. What was observed for the stainless steel was the development of pitting corrosion at ion concentration of $[Cl^-] > 0.6 \text{ mol/dm}^3$, as well as the lack of influence of ion concentration on the repassivation potential.

Keywords: corrosion, stainless steel, titanium alloys, exhaust systems

List of Symbols/Acronyms

b_a, b_c – anodic and cathodic Tafel slopes [$V \cdot \text{dec}^{-1}$];
 E_{cor} – potential of corrosion [V];
 E_{pit} – potential of pitting nucleation [V];
 E_{rp} – repassivation potential [V];
 i_{cor} – current density of corrosion [$\text{mA} \cdot \text{cm}^{-2}$];
 i_{cp} – critical passivation current density [$\text{mA} \cdot \text{cm}^{-2}$];
 i_{pas} – current density of passivation [$\text{mA} \cdot \text{cm}^{-2}$];
 R_p – polarization resistance [$\Omega \cdot \text{cm}^2$];

1. INTRODUCTION

Corrosion of elements of an engine exhaust system has posed a problem for car users since the invention of the first piston engine. The recent years have shown a tendency to reduce mass, extend service time, and improve the quality of components of exhaust systems in mechanical vehicles. Hence the balancing of service time and life of a vehicle or engine that can be observed in the engineering practice when designing the elements and parts of an exhaust system [1-4].

Corrosion of an engine exhaust system is considered on two levels: internal corrosion caused by high temperatures and condensation of exhaust gases, and external corrosion caused by weather conditions, especially salt used during the winter period [5,6]. The intercrystalline, localized, and galvanic corrosion are typical corrosion mechanisms observed in the exhaust systems [3]. One of the basic construction materials used for exhaust systems in

cars are austenitic or ferritic stainless steels [6,7]. These materials are characterized by not only the required mechanical and technological properties, but also good corrosion resistance [8]. Relatively good strength properties and good processability enable producing thin-wall elements out of these alloys, which allows limiting the construction mass. These materials are also characterized by good or limited weldability, as well as the required heat resistance and creep resistance. However, even stainless steel, despite its good or very good corrosion resistance in the exhaust systems, can be subject to damage/ corrosive degradation. The main cause of such damage in the exhaust systems is pitting corrosion, or crevice corrosion, caused by the presence of chloride ions. This type of corrosion results in damages, such as corrosion pits of various depths and uneven local corrosion. [9].

However, titanium and its alloys are materials of lower density than steel, which allows reducing the mass of an entire vehicle, considerably improving the performance of sports cars. At the same time, titanium and its alloys exhibit excellent corrosion resistance in many environments [10-12]. In the presence of oxygen and/or water, titanium passivates spontaneously, as a result of which a thin layer (thickness below 10 nm) of protective oxides appears on its surface [13, 14]. This layer protects the surface of metal from pitting corrosion and crevice corrosion in the presence of halide ions [12]. It is only the influence of strong oxygen acids (e.g. H_2SO_4) or binary acids (e.g. HCl) that lead to active

dissolution of titanium [9,13-16]. Titanium is characterized by higher value of specific strength and specific modulus of elasticity, having better corrosion resistance in comparison with stainless steels [17]. All of the above has an impact on the durability of the whole system, and thus decreases the costs of maintenance and replacement. Titanium exhaust systems are characterized by large capacity, which allows the exhaust gases to flow freely through the whole system easier and faster [18,19].

A variety of factors influencing the corrosion of exhaust systems and the difficult conditions of their service is what makes the wear of exhaust system elements the biggest problem to deal with in the car industry. An exhaust system that is nonfunctional due to corrosion becomes not only a cause of engine failures, but also the source of increasing environmental pollution [20]. Moreover, high thermal efficiency of an engine and extended guarantee periods for new cars make it necessary to analyze the corrosion processes of these elements even more thoroughly.

The paper presents the results of tests and analysis of the external corrosion of the most frequent materials used for the elements of exhaust systems, i.e., stainless steel and titanium. The Authors focused on the role of chloride ions as the products of dissociation of road salt, which is widely used in winter season, and on the influence of their concentration on the corrosion rate of these systems. The internal corrosion, caused mainly by the condensation of exhaust gases with a high content of chlorides and sulfates [21,22], is going to be the subject of the Authors' next research.

2. MATERIAL AND RESEARCH METHODOLOGY

The subjects of the study were samples of materials used in exhaust systems, and these were titanium (grade 3.7035), and stainless steel (grade X5CrNi18-10). The Table 1 presents the chemical composition of the investigated metals.

Table 1. Chemical composition of the materials used for the tests

Materials	Chemical composition, %mass.							
	Ti	C	Nb	Cr	Fe	Ni		
titanium (3.7035)	99.8	0.12	0.011	0.015	0.052	0.02		
X5CrNi18-10		C	Si	Mn	P	S	Cr	Ni
	0.05	0.42	1.64	0.022	0.001	17.5	9.2	

The analysis of chemical composition of the analyzed materials was performed using spark emission spectrometer Bruker Q4 Tasman. Samples in the form of rotating disks with a working surface of 0.2 cm² were used for potentiokinetic tests. The measurements were made with a classic 3-electrode

thermostated measuring vessel, consisting of a working electrode (examined steel), silver-silver chloride reference electrode (AgCl/Ag), whereas the auxiliary electrode was a spiral-shaped platinum wire.

All measurements were performed at a temperature of 25 ± 0.1°C, with a disk rotation speed of 12 rps rotations per second and a potential scanning speed of 10 mV·s⁻¹. The general corrosion resistance was assessed by plotting a full potentiokinetic curve in the range from -1.0 to +1.9V in an aerated 0.5M Na₂SO₄ solution, acidified (by the addition of sulfuric acid H₂SO₄) pH=2.0. In order to determine the susceptibility of materials to pitting corrosion, the 0,5M solutions of Na₂SO₄ were applied, containing an addition of Cl⁻ ions of 0,2-1,0M concentration. These solutions were acidified to the value of pH = 2 by adding to them solutions of the same ionic strength consisting of Na₂SO₄, H₂SO₄ and NaCl. To determine the values of pit nucleation potentials (E_{pit}), the method of unidirectional polarization curves was used, starting their registration from the cathodic $E_{start} = -0.5V$ values and ending the measurement after the passive layer was broken through and the anodic current reached a value of several mAcm⁻². To determine the repassivation potential (E_{rp}), bidirectional waveforms were used, recording curves in the anodic range and reversing the direction of the potential shift after reaching the anodic breakdown current of 10 mA·cm⁻². Reversing the direction of the potential shift initially resulted in a further increase in the anodic current, and then its rapid decrease. The point of intersection of the return curve with the increasing curve in the passive range was taken as the repassivation potential, analogously to the method described in the works [23,24]. The record of polarization curves was made by the electrochemical measuring station CHI 130 (CH Instruments, USA) connected to a computer and compatible with the computer software, the each measurements was repeated three times. The test samples of austenitic steel and titanium prepared for the corrosion test were characterized by the following values of roughness parameter R_a and R_z , respectively: 14.23 and 71.65 μm (for austenitic steel), and 20.48 and 173.07 μm (for titanium).

The metallographic studies were carried out using optical (Keyence VHX 7000) and scanning electron (Jeol 6610 LV) microscopes. The surface of the analyzed materials was observed after corrosion tests in environments with different concentrations of chloride ions.

3. RESULTS AND DISCUSSION

The polarization curves of titanium and austenite stainless steel recorded after the test in a 0.5 M Na₂SO₄ solution acidified to pH = 2.0 and the values of polarization resistance determined on their basis,

which is a measure of the corrosion rate, are shown in Figure 1.

The course of the polarization curves (Fig. 1) indicates that both stainless steel and titanium have very good corrosion properties in the corrosive environment used. For both tested materials, a wide range of potentials is observed on the anode side, in which a passive state occurs, and the measured current density remains constant despite the increasing potential. A higher value of the corrosion potential (E_{cor}) and lower values of anode currents indicate that the material is characterized by higher resistance to a corrosive environment [25].

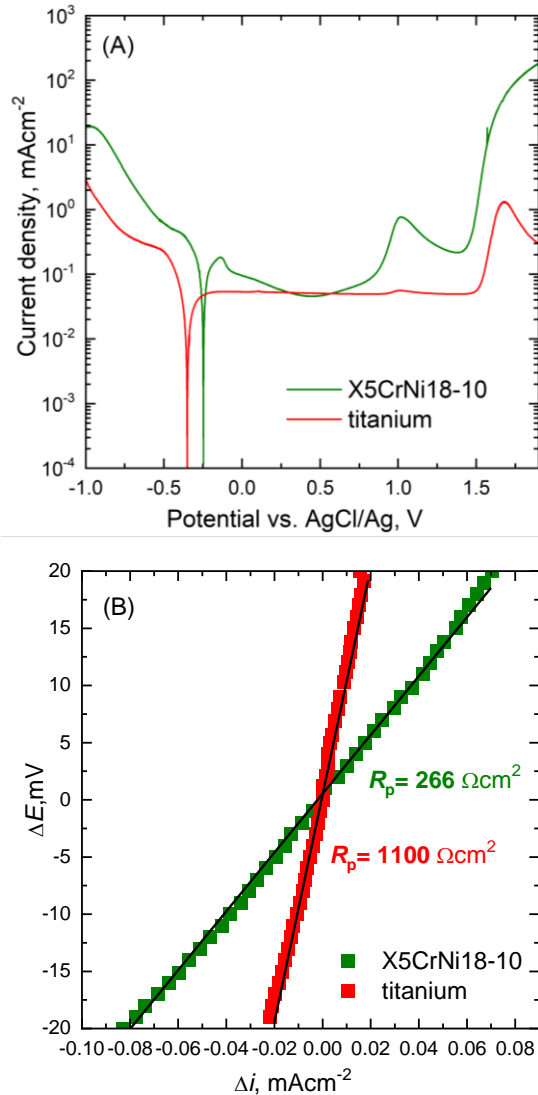


Fig. 1. Potentiokinetic polarization curves for stainless steel and titanium (A) and measurements of linear polarization $\Delta E = E - E_{cor} = f(i_{out})$ for these materials (B). Experimental conditions: 0.5M Na₂SO₄ (pH = 2.0), 10 mV·s⁻¹, 12 rps.)

Stainless steel, despite the later transition to the active state (higher E_{cor} value than for titanium), shows slightly higher i_{cp} values, the value of which indicates a slightly more difficult transition to the passive state. This material also has a narrower range of potentials at which the passive layer is stable.

From a potential value higher than approximately 0.75V, a transition of the stainless steel surface into the transpassive range is observed, associated with the reconstruction and weakening of the protective properties of the oxide layers (Fig. 1). In turn, the tested titanium alloy is characterized by high stability of the passive layer.

As can be seen from Fig. 1A, in the corrosive environment used, this material easily turns into a passive state, and the anode current remains at a constant, low level up to a potential value of approximately 1.5V. Above the value of this potential, an increase in the anodic current can be seen, related to the change in the oxidation degree of titanium in the passive layer: from degree +II (TiO) to degree +IV (TiO₂) - characteristic for both pure titanium and alloys based on it [26].

Fig. 1B shows the linear polarization dependences $\Delta E = E - E_{cor} = f(i_{out})$ for potentials equal to E_{cor} , according to the Stern-Hoar equation [27] the slope of the appropriate lines is a measure of the polarization resistance (R_p). In turn, the inverse of R_p is proportional to the corrosion current density:

$$i_{cor} = \frac{b_a \cdot b_c}{b_a + b_c} \cdot \frac{1}{2.3 R_p} \quad (1)$$

In our case, formally assuming $b_a = \infty$ and $b_c = 0.12V$, we find:

$$i_{cor} = \frac{0.052}{R_p} \quad (2)$$

Characteristic electrochemical quantities read from the polarization curves (Fig. 1A) and the values of the resistance of polarization R_p are listed in Table 2.

Table 2. Corrosion resistance parameters of stainless steel and titanium in a 0.5M H₂SO₄ (pH = 2.0) environment

	E_{cor} [V]	i_{cp} [mA· cm ⁻²]	i_{pas} [mA· cm ⁻²]	R_p [Ω·cm ²]	i_{cor} [mA· cm ⁻²]
X5CrNi 18-10	-0.25	0.20	0.05	266	0.20
Ti-alloy	-0.35	0.05	0.05	1100	0.05

To assess the susceptibility of the tested materials to pitting corrosion, a series of polarization curves were prepared in 0.5M sulfate solutions containing 0.2-1.0 mol/dm³ of [Cl⁻] ions. The corresponding polarization curves for titanium and stainless steel are shown in Fig. 2.

The polarization curves confirmed titanium's high resistance to pitting corrosion (Fig. 2A). At the concentrations of chloride ions used in the experiment, no significant impact on the course of the curves in the passive range was observed (E_{pit}). Therefore, no damage to the oxide layer and the associated characteristic breakdown potential are observed. The only changes in the course of the curves are observed only above the potential $E = 1.5V$ when the passive layer on the titanium surface

is rebuilt. A slight decrease in current values in this area suggests that the presence of chlorine ions in the corrosive environment facilitates the change in the oxidation state of titanium in the passive layer.

Despite its corrosion resistance, stainless steel is not as resistant to chloride ions as titanium. In Hanks' solution, the potential of pit nucleation or so called breakdown potential (E_{pit}) for titanium alloy is 1.9 V while for austenitic stainless steel it is 0.28 V [28].

The course of the potentiokinetic curves for stainless steel in environments with different concentrations of chloride ions is shown in Figure 2B and 3. A systematic increase in the concentration of $[Cl^-]$ ions in the solution facilitates the nucleation of pits, and therefore the breakdown potential takes lower values. However, no significant effect of chloride ion concentration on the repassivation potential was observed in the solutions used. It assumes very similar values independently for all $[Cl^-]$ ion concentrations used (Fig. 3).

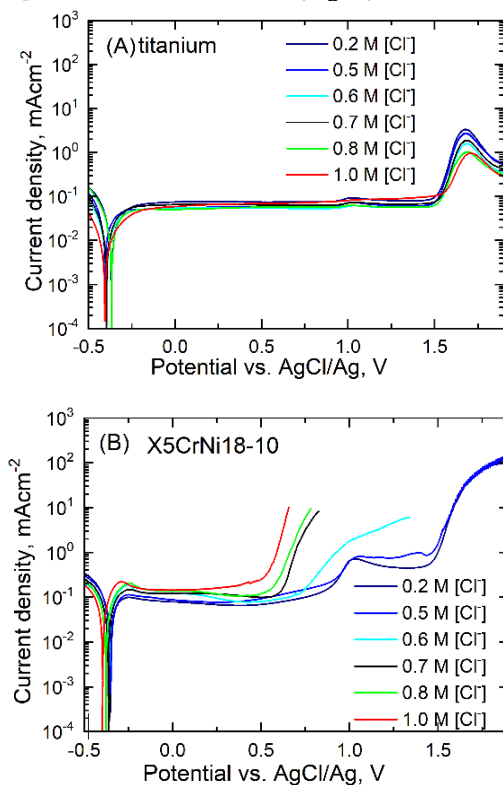


Fig. 2. Potentiokinetic polarization curves made for titanium (A) and the XCrNi18-10 alloy (B) in an acidified sulfate environment containing various concentrations of chloride ions

In the case of stainless steel, reversing the direction of potential shift, after reaching the anode current of approximately $10 \text{ mA}\cdot\text{cm}^{-2}$, initially causes a further increase in current density (Figs. 3). It should be noted, however, that above E_{pit} the curve for the concentration of $0.6 \text{ M } [Cl^-]$ shows the lowest steepness, which indicates a low rate of pit development in this environment. However, the steepness of the curves for higher concentrations of chloride ions is much greater, which is the result of the intensive process of pit development. The

thermodynamic susceptibility of a material to pitting corrosion is greater, the lower the pit nucleation potential [29].

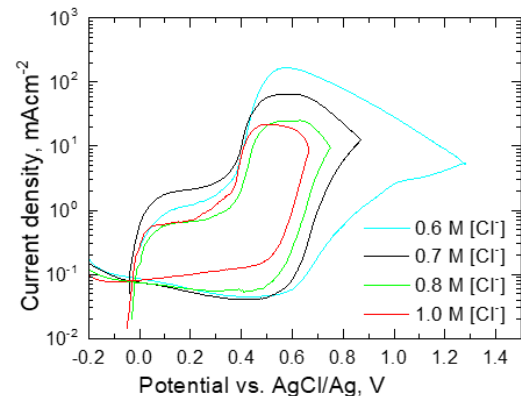


Fig. 3. Potentiokinetic polarization curves of XCrNi18-10 stainless steel determined by the method of cyclic polarization in an acidified sulfate environment containing various concentrations of chloride ions. Experimental conditions: $0.5 \text{ M Na}_2\text{SO}_4$ ($\text{pH} = 2.0$), $10 \text{ mV}\cdot\text{s}^{-1}$, 12 rps.

For all analyzed concentrations of $[Cl^-]$ ions, the decrease in current density is visible only from a potential of approximately 0.45 V . Additionally, in the last stage of recording the curves, their courses are so convergent that no differences in the repassivation potential values are observed. Images of the stainless steel surface taken after exceeding the E_{pit} potential and reaching a current of approximately $10 \text{ mA}\cdot\text{cm}^{-2}$ and at a potential of 0.45 V after exposure to a sulphate solution containing $1.0 \text{ M } [Cl^-]$ ($\text{pH} = 2.0$) are shown in Fig. 4(A- B). In turn, Fig. 4C shows a pit-free surface of a titanium alloy after a corrosion test in the same environment for comparison.

After the corrosion test, despite the reversal of the direction of the potential, both the number of pits and their size increase intensively (Fig. 4A-B).

It should be emphasized, however, that despite the reduced resistance of the material to the rate of pit development with the increase in the aggressiveness of the environment, the value of the repassivation potential remains unchanged. The constancy of E_{rp} results in lower potential-current hysteresis for environments for which the breakdown potential is the lowest. As previous works of the authors show [10,11], the smaller the $E_{pit} - E_{rp}$ difference, the lower the material wear caused by pitting corrosion.

Typical surface of the stainless steel after a full corrosion test in a solution of minimum (Fig.5A) and maximum (Fig.5B) chloride ion concentration is presented in Figs. 5a and 5b, respectively. Figs. 6 and 7 present examples of width and depth of the pits after the performed corrosion tests.

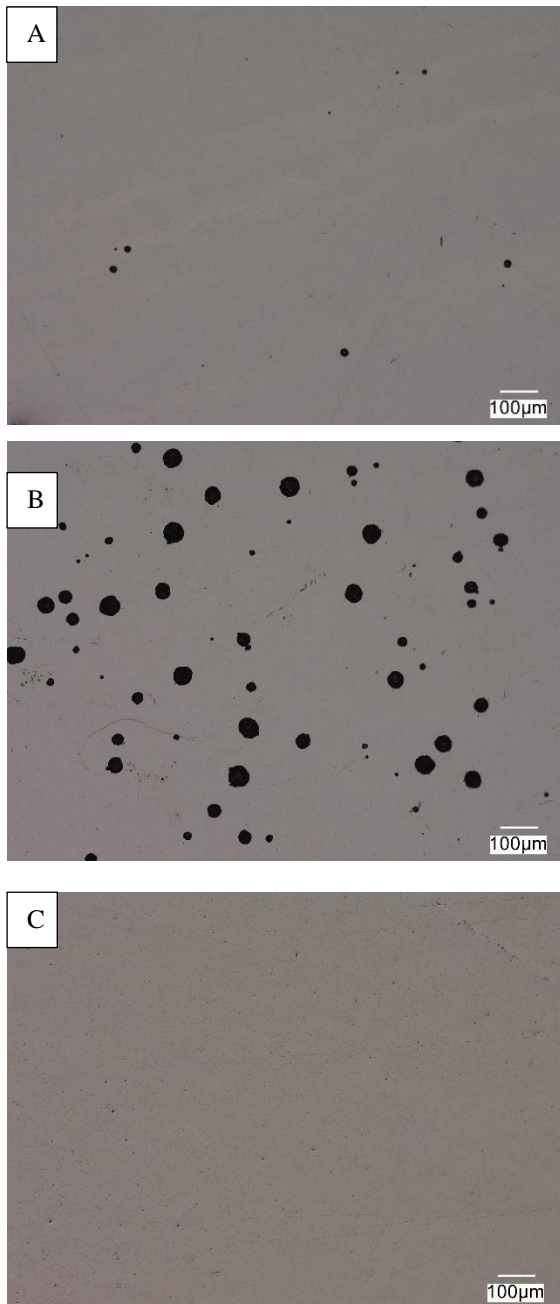


Fig.4. The surface of the samples after the corrosion test in 0,5M Na₂SO₄ (pH = 2.0) + 1.0 M [Cl⁻] (pH = 2.0), characteristic for a current density of approximately 10 mA·cm⁻² (A) and a potential $E = 0.45V$ (B) for stainless steel and for a titanium alloy (C)

An increase in the concentration of chloride ions favored the nucleation of pits, contributing to the increase in their number on the analyzed surface (Fig. 5). The growth of the number of pits, however, does not go together with the growth of their width and depth. As proved by the measurements of pits width after exposure to 0.6M [Cl⁻] (Fig. 6), the dominant pits were above 120 µm wide, and most of them were more than 60 µm deep. Meanwhile, on the surface of test pieces after exposure to solution containing 1.0M chloride ions the width ranged between 17 µm and 45 µm, and their depth was

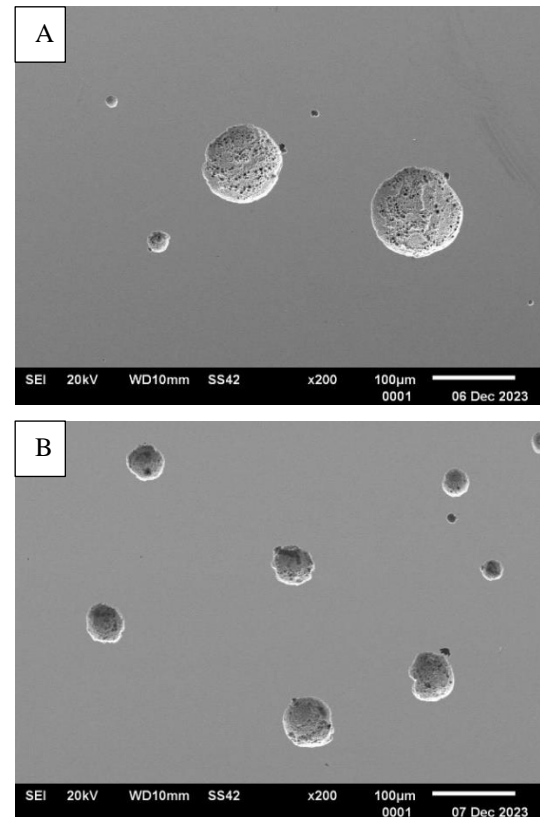


Fig.5. The surface of the samples after the plotting the full polarization curve in sulphate solution containing (A): 0.6 M [Cl⁻] and (B): 1.0 M [Cl⁻].

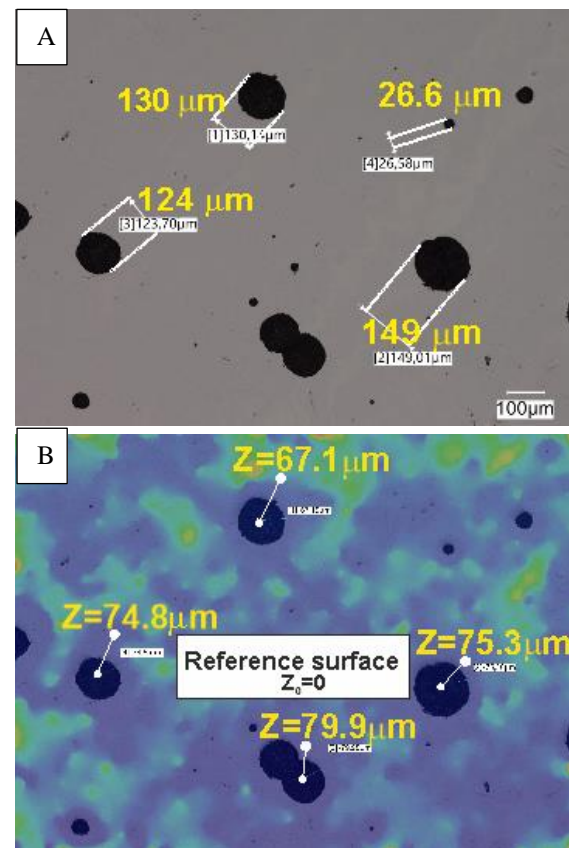


Fig. 6. Pits depth (A) and width (B) of stainless steel after corrosion test in sulphate solution containing 0.6 M [Cl⁻]

estimated at around 3-5 μm (Fig. 7). This fact proves earlier observations that pits are easier to initiate and spread at the higher concentration of chloride ions, however, it does not result in the material being etched out inside those pits.

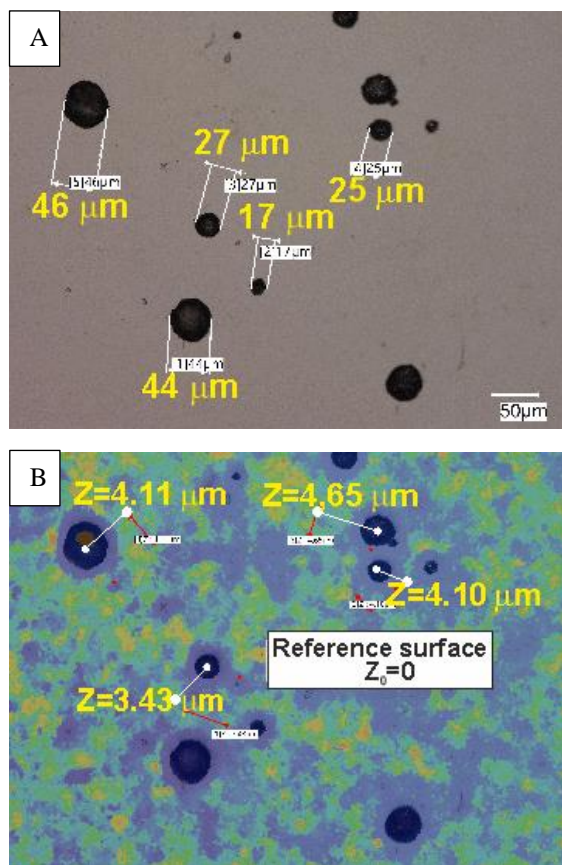


Fig. 7. Pits depth (A) and width (B) of stainless steel after corrosion test in sulphate solution containing 1.0 M [Cl⁻]

4. SUMMARY

As proved in the research carried out, both the stainless steel X5CrNi18-10 used for exhaust system elements and titanium 3.7035 show very good corrosion resistance in acidic environment without [Cl⁻] ions.

The contact of exhaust systems with corrosive environment containing chloride ions, whose presence on roads is connected with removal of icing, favours their corrosive wear. In the applied range of [Cl⁻] concentrations the stainless X5CrNi18-10 steel showed resistance to the local attack of chlorides up until the concentration equal to 0.6 mol·dm⁻³. For higher concentrations, the development of pitting corrosion was observed on the steel surface, reflected in a decrease of E_{pit} as the environment aggressiveness was growing. Such behaviour was not observed for the examined titanium, which showed complete resistance to the ions [Cl⁻] for the whole range of their concentrations.

The influence of chloride ions concentration on the repassivation potential (E_{rp}) of the examined

stainless steel was not observed. The consequence of the above was a decrease in the difference between E_{pit} and E_{rp} , as well as lower wear of the material resulting from pitting corrosion. In this context, the damages of surface caused by corrosion should not grow rapidly, despite the increasing susceptibility to pitting corrosion as the corrosive aggressiveness of the environment grows.

Source of funding: *This research received no external funding.*

Author contributions: *research concept and design, K.J-W., G.G.; Collection and/or assembly of data, K.J-W., G.G.; Data analysis and interpretation, K.J-W., G.G.; Writing the article, K.J-W., G.G.; Critical revision of the article, K.J-W., G.G.; Final approval of the article, K.J-W., G.G.*

Declaration of competing interest: *The authors declare that they have no known competing financial interests or personal relationships that could have appeared to influence the work reported in this paper.*

REFERENCES

- Gümpel P, Schiller D, Arlt N, Bouchholz D. Simulation of corrosion behaviour of stainless steels in passenger car exhaust systems. *ATZ worldwide* 2004; 106(4): 18–20. <https://doi.org/10.1007/BF03224662>.
- Wei Z. Characterization of materials for exhaust systems under combined mechanical and corrosive environment. 2013-01–2420. c
- Chang S, Jun JH. Corrosion resistance of automotive exhaust materials. *Journal of Materials Science Letters* 1999; 18(5): 419–21. <https://doi.org/10.1023/A:1006613624476>.
- Kim MJ, Jang SI, Woo SH, Kim JG, Kim YH. corrosion resistance of ferritic stainless steel in exhaust condensed water containing aluminum cations. *Corrosion* 2015; 71(3): 285–91. <https://doi.org/10.5006/1408>.
- Doche ML, Hihn JY, Mandroyan A, Maurice C, Hervieux O, Roizard X. A novel accelerated corrosion test for exhaust systems by means of power ultrasound. *Corrosion Science* 2006; 48(12): 4080–93. <https://doi.org/10.1016/j.corsci.2006.04.009>.
- Yasir M, Mori G, Wieser H, Schattenkirchner M, Hög M. A new testing method for lifetime prediction of automotive exhaust silencers. *International Journal of Corrosion* 2011; 2011: 1–5. <https://doi.org/10.1155/2011/689292>.
- Chang S, Jun JH. Corrosion resistance of automotive exhaust materials. *Journal of Materials Science Letters* 1999; 18: 419–421. <https://doi.org/10.1023/A:1006613624476>.
- Lippold JC, Kotecki DJ. *Welding metallurgy and weldability of stainless steel*. Wiley-Interscience 2005.
- Hoffmann C, Gümpel P. Pitting corrosion in the wet section of the automotive exhaust systems. *Journal of Achievements of Materials and Manufacturing Engineering* 2009; 34(2): 115–121.
- Lavrenko VA, Shvets VA, Makarenko GN. Comparative study of the chemical resistance of titanium nitride and stainless steel in media of the oral cavity. *Powder Metallurgy and Metal Ceramics* 2001;

- 40(11/12): 630–6.
<https://doi.org/10.1023/A:1015296323497>.
11. Utomo WB, Donne SW. Electrochemical behaviour of titanium in H₂SO₄–MnSO₄ electrolytes. *Electrochimica Acta* 2006; 51(16): 3338–45. <https://doi.org/10.1016/j.electacta.2005.09.031>.
 12. Gurrappa I. Characterization of titanium alloy Ti-6Al-4V for chemical, marine and industrial applications. *Materials Characterization* 2003; 51(2–3): 131–9. <https://doi.org/10.1016/j.matchar.2003.10.006>.
 13. Donachie MJ. Titanium - A technical guide, 2nd Edition. ASM International 2000.
 14. Muñoz-Portero MJ, García-Antón J, Guiñón JL, Leiva-García R. Pourbaix diagrams for titanium in concentrated aqueous lithium bromide solutions at 25°C. *Corrosion Science* 2011; 53(4): 1440–50. <https://doi.org/10.1016/j.corsci.2011.01.013>.
 15. Noël JJ, Ebrahimi N, Shoesmith DW. Corrosion of titanium and titanium alloys. *Encyclopedia of Interfacial Chemistry* 2018 s. 192–200. <https://doi.org/10.1016/B978-0-12-409547-2.13834-X>.
 16. Khoma MS, Pomaniv OM, Kuntiyi OI, Tymchyshyn AI. Anodic behaviour of titanium in acid sulfate electrolytes for copper plating. *Materials Science* 2000; 36(5): 780–3. <https://doi.org/10.1023/A:1011332513343>.
 17. Aragon E, Woillez J, Perice C, Tabaries F, Sitz M. Corrosion resistant material selection for the manufacturing of marine diesel exhausts scrubbers. *Materials & Design* 2009; 30(5): 1548–55. <https://doi.org/10.1016/j.matdes.2008.07.053>.
 18. Idzior M, Karpiuk W, Bor M, Smolec R. Modern solutions used in motorcycle engines. *Autobusy* 2017; 6: 743-748.
 19. Muslim MT, Selamat H, Alimin AJ, Mohd Rohi N, Hushim MF. A review on retrofit fuel injection technology for small carburetted motorcycle engines towards lower fuel consumption and cleaner exhaust emission. *Renewable and Sustainable Energy Reviews* 2014; 35: 279–84. <https://doi.org/10.1016/j.rser.2014.04.037>.
 20. Šolic T, Maric D, Suhi S, Samardžic I. Analysis of the vehicle exhaust system corrosion and its effect on the eco-test result. *Metalurgija* 2022; 61(3-4): 841-844.
 21. Gazdowicz J, Radwański K, Rybarz M. Influence of exhaust system operating conditions on corrosion of high-alloy ferritic steel silencer jackets. *Prace Instytutu Metalurgii Żelaza* 2007; 59(3): 24-30.
 22. Żaba K, Nowak S, Kąc S. Examinations of corrosion resistance Al-Si coated tubes to be used as elements of exhaust systems. *Laboratory researches. Rudy i Metale Nieżelazne* 2005; 50(12): 679-685.
 23. Jagielska-Wiaderek K. Structure of outer layer of stainless steels after high-temperature chemical treatments and their susceptibility to local corrosion. *Ochrona przed Korozją* 2012; 11: 491-494.
 24. Bala H, Giza K, Jagielska K. Evaluation of pitting corrosion development using bi-direction polarization technique. *IXth International Corrosion Symposium and Exhibition Ankara, ICCP Proceedings* 2004; 1: 123-128.
 25. Perez N. *Electrochemistry and Corrosion Science* Springer 2016. <https://doi.org/10.1007/978-3-319-24847-9>.
 26. Brojanowska A, Ossowski M, Sobiecki JR, Wierzchoń T. Corrosion resistance in Ringer solution of titanium alloy Ti6Al4V after low-temperature glow-discharge

nitriding and carbonitriding. *Inżynieria Materiałowa* 2008; 6: 963-966.

27. Richardson TJA. *Shreir's Corrosion*. 1st Edition, Elsevier – Acad. Press 2009.
28. Leda H. *Materiały inżynierskie w zastosowaniu biomedycznym*. II Eds. Wydawnictwo Politechniki Poznańskiej 2012.
29. Szklarska-Smiałowska Z. *Pitting and Crevice Corrosion*. NACE International, Houston 2005.



Dr inż. Karina JAGIELSKA-WIADEREK

Was graduated from the Czestochowa University of Technology in the direction of Materials Engineering. Currently employed as assistant professors at the Department of Materials Engineering, Czestochowa University of Technology. Her main fields of

interest include: corrosion of metals and alloys, electrochemistry and surface engineering.

e-mail: k.jagielska-wiaderek@pcz.pl



Prof dr hab. inż. Grzegorz GOLĄŃSKI

Was graduated from the Czestochowa University of Technology in the direction of Materials Engineering. Currently employed as assistant professors at the Department of Materials Engineering, Czestochowa University of Technology. His main fields of scientific research include: steel, alloys, heat

treatment, mechanical properties.

e-mail: grzegorz.golanski@pcz.pl